On the X-ray Baldwin Effect in Active Galactic Nuclei Observed by the *Chandra* High Energy Grating

X. W. Shu[1], J. X. Wang[1], T. Yaqoob[2], P. Jiang[1], Y. Y. Zhou[1]

ABSTRACT

Using *Chandra* High Energy Grating (HEG) observations of 32 AGNs, we present a systematic study of the X-ray Baldwin effect (XBE, i.e. the anti-correlation between narrow Fe Kα line EW and X-ray continuum luminosity for AGN samples) with the highest spectral resolution currently available. We have previously reported an anti-correlation with $EW \propto L_{2-10\ \mathrm{keV}}^{-0.22}$ in a HEG sample, and the correlation is much weaker after averaging multiple observations of individual AGNs ($EW \propto L_{2-10\ \mathrm{keV}}^{-0.13}$). This indicates that rapid variation in X-ray continuum plays an important role in producing the XBE, and such an effect should also be visible in individual AGNs. In this paper, by normalizing the line EWs and continuum luminosities to the time-averaged values for each AGN in our sample with multiple HEG observations, we find a strong anti-correlation between EW and L_X ($\mathrm{EW}/\langle EW\rangle \propto (L/\langle L\rangle)^{-0.82\pm0.10}$), consistent with the XBE expected in an individual AGN if the narrow line flux remains constant while the continuum varies. This is first observational evidence that the Fe Kα line flux in a large sample of AGNs lacks of a corresponding response to the continuum variation, supporting that the narrow Fe-K line emission originates from a region far from the nucleus. We then performed Monte-Carlo simulations to address whether the global XBE can be produced by X-ray continuum variation solely, and found that such interpretation of XBE cannot be ruled out statistically. One thus should be very cautious before reaching any scientific conclusion based on an observed XBE.

Subject headings: galaxies: active — line: profile — X-rays: galaxies

[1] CAS Key Laboratory for Research in Galaxies and Cosmology, Department of Astronomy, University of Science and Technology of China, Hefei, Anhui 230026, P. R. China, xwshu@mail.ustc.edu.cn, jxw@ustc.edu.cn

[2]Department of Physics and Astronomy, Johns Hopkins University, Baltimore, MD 21218, yaqoob@pha.jhu.edu

1. INTRODUCTION

The narrow (FWHM $< 10,000$ km s^{-1}) Fe Kα fluorescent emission at ~ 6.4 keV is a common feature in the X-ray spectra of active galactic nuclei (AGN) (e.g. Sulentic et al. 1998; Lubiński & Zdziarski 2001; Weaver, Gelbord, & Yaqoob 2001; Perola et al. 2002; Yaqoob & Padmanabhan 2004; Bianchi et al. 2007; Winter et al. 2009; Shu, Yaqoob & Wang 2010 (hereafter Paper I); Fukazawa et al. 2011). Such a narrow Fe Kα line is believed to be produced in cold, neutral matter far from the nucleus (see Paper I, and references therein). Possible origins of the Fe Kα line include the outer regions of an accretion disk, the broad-line region (BLR), and a parsec-scale torus (Nandra 2006; Bianchi et al. 2008; Paper I; Liu & Wang 2010; Shu, Yaqoob & Wang 2011; Jiang, Wang & Shu 2011). In some cases, the line has been resolved by the *Chandra* high-energy grating (HEG; see Markert et al. 1995) with FWHM typically less than 5000 km s^{-1} (e.g. Kaspi et al. 2000; Yaqoob et al. 2001; Paper I; Shu et al. 2011). In Paper I, we measured the intrinsic width of the narrow Fe Kα line core in a large sample of type I AGNs using the *Chandra* HEG, and obtained a weighted mean of FWHM=2060 $\pm$ 230 km s^{-1}. Interestingly, this width of the line is fully consistent with that obtained in type II AGNs observed with *Chandra* HEG (Shu et al. 2011), indicating a common origin of the narrow Fe Kα line in both AGN populations.

The equivalent width (EW) of the Fe Kα line was found to be anti-correlated with the X-ray continuum luminosity (also known as X-ray Baldwin effect) in several AGN samples (e.g., Iwasawa & Taniguchi 1993; Nandra et al. 1997b; Page et al. 2004; Jiang, Wang, & Wang 2006; Bianchi et al. 2007; Winter et al. 2009; Chaudhary et al 2010). Note the observed X-ray Baldwin effect in some samples could be (at least) partly due to the contamination of radio-loud objects (Jimenéz-Bailón et al. 2005; Jiang et al. 2006). It is also interesting to note a recent work by Krumpe et al. (2010) who found that the X-ray Baldwin effect flattens above $L_X \sim 10^{44}$ erg s^{-1}, claiming that the anti-correlation (if exists) is only relevant in radio-quiet AGNs with $L_X < 10^{44}$ erg s^{-1}.

There are several physical factors that could produce the X-ray Baldwin effect. One possibility is that the covering factor and/or the column density of line-emitting material decreases with increasing X-ray continuum luminosity (e.g., Page et al. 2004). Alternatively, the X-ray Baldwin effect could be artificial due to the rapid X-ray continuum variation in AGNs. Jiang et al. (2006) reported that X-ray continuum variation model can naturally produce a global X-ray Baldwin effect in their composite Chandra/XMM sample. In Paper I, with Chandra HEG data, we also found that averaging multiple observations of individual sources could significantly smear the X-ray Baldwin effect from $EW \propto L^{-0.22}$ to $EW \propto L^{-0.13}$. This clearly indicates that the observed X-ray Baldwin effect could at least partially attributed to continuum variation.

Another possibility is contamination from the Fe Kα line emission from the accretion disk, which could be more and more ionized as the X-ray luminosity increases, leaving less low-ionization material to produce the Fe Kα line at $\sim$ 6.4 keV (e.g., Nandra et al. 1997b; Guainazzi et al. 2006; Nayakshin 2000a, 2000b). Therefore, it is essential to study the X-ray Baldwin effect for narrow Fe K line emission with the highest spectral resolution available, to isolate the narrow cores from the broad component.

Using a sample that consists only of HEG data[1], we can investigate the X-ray Baldwin effect with a spectral resolution in the Fe K band that is nearly four times better than in previous studies that relied on CCD data (or data with a resolution worse than CCDs), and therefore provide the best isolation of the narrow core that is currently possible. In this paper, we extend the results of Paper I to investigate the origin of the Baldwin effect, in particular taking into consideration of the effect of X-ray continuum variability. Throughout this paper, we adopt a cosmology of $\Omega_M = 0.3, \Omega_\lambda = 0.7$, and $H_0 = 70$ km s^{-1} Mpc^{-1}.

2. OBSERVATIONS AND SPECTRAL FITTING

Our study is based on data from 85 *Chandra HETGS* observations of 32 AGNs that are known to have X-ray absorbing column densities ($N_{\rm H}$) less than 5×10^{22} cm^{-2}, as of 2010 Aug 1, filtering on several criteria as shown in Paper I . Note that heavily absorbed AGNs were excluded because their X-ray spectra are too complex, and the measurements of the narrow Fe Kα line and intrinsic continuum luminosities in such sources can become model dependent. Except for 15 new observations for NGC 4051 and Ark 564, all the data are taken from Paper I. We excluded 4 radio-loud objects (3C 120, 3C 273, 3C 382 and 4C 74.26) from our analysis, because their X-ray spectra might be contaminated by the relativistic jet. The *Chandra* data for the sample were reduced and HEG spectra were analyzed as described in Yaqoob et al. (2003). Further details of the *Chandra* HEG data can be found in Paper I. Note that in our analysis, we fixed the emission-line width, $\sigma_{\rm FeK}$, at 1 eV (corresponding to $\sim$ 100 km s^{-1} FWHM at 6.4 keV), a value well below the HEG resolution, in order to obtain a uniform measurements of the narrowest, unresolved core component of the Fe Kα line for all the data sets.

[1] *Chandra* HEG affords best spectral resolution currently available in the Fe K band, at 6.4 keV is $\sim$39 eV, or $\sim$1860 km s^{-1} FWHM.

3. RESULTS AND DISCUSSIONS

In Paper I, we studied the correlation between the EW of the Fe Kα line and the 2–10 keV continuum luminosity ($L_{\rm x}$) for the measurements from individual observations ("*per observation*" sample), and from individual sources ("*per source*" sample)[2], respectively. Despite better isolation of the Fe Kα line core, there is still an anti-correlation between the EW and the X-ray luminosity in the diagrams (Figure 7 in Paper I). In this paper, we first present a similar analysis of the anti-correlation, this time including 15 new *Chandra* HEG observations. We found a similar result that the "*per observation*" sample gave a stronger anti-correlation ($\alpha = -0.18 \pm 0.03$) than the "*per source*" sample ($\alpha = -0.11 \pm 0.03$). Quantitatively, the anti-correlation for the"*per observation*" results is significant at a level of $\sim 6.39\sigma$, as opposed to $\sim 3.74\sigma$ for the "*per source*" results for a non-zero slope.

3.1. Fe Kα Line Baldwin Effect in Individual Sources

As we discussed in Paper I, the weaker anti-correlation (in the slope) in the "*per source*" sample could be due to the obvious reduction of the EW variability when data from multiple HEG observations were averaged. This clearly indicates that rapid variation in X-ray continuum plays an important role in producing the XBE, and such an effect should also be visible in individual AGNs.

In fact, the Fe Kα line EW in an individual source can vary by more than a factor of two. For example, from Table 1 in Paper I, we can see that in five observations of NGC 4151, while the line intensity does not show significant variation, the continuum changes by a factor of $\sim$4 can lead to a change in the EW by a factor of $\sim$3-4. In Figure 1, we plot the 13 *Chandra HETGS* observations of NGC 4051 and the best-fit line for the correlation. We find clearly a decrease in the EW as the luminosity increases, an inverse correlation with $EW \propto L^{-0.75\pm0.60}$. Note that the slope cannot be well determined (the significance for the anti-correlation is only at a level of 1.24σ), possibly due to the limited number of exposures and the large measurement errors in Fe Kα line EW.

To make full use of multiple Chandra HEG observations on individual AGNs, we plot in Figure 2 the EW of the Fe Kα line against the 2-10 keV luminosity for all sources which were observed by *Chandra* HEG more than once. Both the EW and the X-ray luminosity were normalized by the time-averaged values for each source. The averaged EW ($\langle$EW$\rangle$)

[2]Measurements for the latter were derived from only one spectrum per source, which in some cases was the time-averaged spectrum of multiple observations, as described in Paper I.

and X-ray luminosity ($\langle L_x \rangle$) are the best-fitting values from the spectrum averaged over multiple observations of a source where relevant. It can be seen that there is clearly an inverse correlation between the normalized EW and luminosity in log-log space, thanks to our large sample of the HEG observations. Using a similar fitting method as in Paper I, we find the anti-correlation is significant at a level of $\sim 7.8\sigma$, and the best-fitting slope of the correlation is –0.82±0.10, a value very close to –1 within the uncertainties. A slope of –1 could be expected if the Fe Kα flux in an individual AGN remains constant, since the EW was calculated by the flux of the Fe Kα line over the continuum at ~ 6.4 keV. Note the slight deviation of the best-fit slope from –1 (see Figure 2) could be due to the less variable EW of the Fe Kα line than the 2-10 keV continuum. This is possibly because of spectral variability in some AGNs where the X-ray spectra soften as they brighten (with the relatively softer energies displaying stronger variability, see e.g., Markowitz & Edelson 2004), so that the continuum variation amplitude at ~ 6.4 keV could be smaller than that in the 2-10 keV. On the other hand, if there is an underlying broad Fe Kα line component, it may affect the EW of the narrow line. However, a broad-line component is difficult to deconvolve with the HEG. This problem was addressed in Yaqoob et al. (2001) who found that the effect of an underlying broad line on the EW of the narrow line, with parameters that are typical of type 1, is of the order of a few percent. Since the narrow line dominates over the broad line even more in type 2 AGN, the effect is even less significant.

Another factor affecting the anti-correlation above could be the uncertainty in the X-ray continuum determination. The 2-10 keV continuum luminosities shown in Figure 2 were obtained by extrapolating the best-fitting model up to 10 keV, which could give inaccurate luminosities if the continuum shape is significantly different in the 7-10 keV band compared to the extrapolated model. We performed simulations of 0.5–10 keV HEG spectrum based on the NGC 3783 data (the deepest observation with HEG) with a complex model including a partially covered absorption, a thermal black body for the soft excess, a power law and a Compton reflection component and both broad and narrow Fe Kα lines[3]. Using the simulated spectrum as input, we then fitted the 2-7 keV HEG data with the empirical power-law model as in Paper I and obtained the extrapolated 2-10 keV flux. We found a value is comparable with the input one, with a difference in the 2-10 keV X-ray flux of the order of 6%. In addition, we also performed spectral fitting to the broad-band *Suzaku* spectrum (0.5–50 keV) for one of our objects (F9), and compared the best-fitted 2-10 keV flux to that by extrapolating with the empirical model. We found that the difference in flux is less than 1%.

[3]In this model, we assumed a most complex continuum for AGNs in current sample, with absorption $N_H = 10^{23}$ cm^{-2} and Compton reflection component $R = 4$. The broad Fe K Gaussian line was assumed to have $E = 5.9$ keV, $\sigma = 0.7$ keV and $EW = 200$ eV (the values for MCG -6-30-15, e.g., Nandra et al. 2007).

We therefore conclude that the effect of the continuum slope at $\sim$ 7–10 keV on the values of the extrapolated X-ray luminosities is unimportant.

3.2. Simulating the Global X-ray Baldwin Effect

Assuming constant Fe Kα line flux, Jiang et al. (2006) studied that whether the variability of the X-ray continuum alone can account for the global X-ray Baldwin effect observed in their Composite Chandra/XMM sample. Although having a large scatter, they found that the simulated anti-correlation has a slope of -0.05 ± 0.05, and 8.4% of the simulations could produce anti-correlation steeper than the observed ones. We checked this possibility for our *Chandra* grating sample by simulating the variability of the EW that is caused by the X-ray continuum variations. The amplitude of the X-ray continuum variation can be quantified by calculating the fractional variability amplitude, $F_{\rm var}$ (e.g., Nandra et al. 1997a), which is simply the square root of the normalized excess variance ($\sigma^2_{\rm NXS}$), taking into account Poisson noise.

In our simulations, we first adopted a similar time variation model as Jiang et al. (2006), that the observed X-ray luminosity is normally distributed with the Gaussian width being the fractional variability amplitude, using the correlation $F_{\rm var} \propto L_{\rm X}^{-0.135}$ of Markowitz & Edelson (2004) for the longest timescale data (1296 days, $\sim$3.5 yr). Note that the use of the timescale of years is motivated by the fact that it corresponds to the expected light-crossing time of the region producing the narrow Fe K line emission (see Shu et al. 2011).

For comparison, we also computed the observed excess variance for our sources with multiple HEG observations, based on the data from Figure 2. All sources were assumed to have an uncertainty in the continuum luminosity measurement, typically $\sim$2% at 68% confidence level. We obtained $\sigma^2_{\rm NXS} = 0.054 \pm 0.012$, corresponding to a fractional variability amplitude $F_{\rm var} = 23.3\%$. This is comparable with but smaller than the mean $F_{\rm var}$ of 33.3% calculated from the employed time variation model, likely due to the fact that many of the multiple HEG observations spans a much shorter time scale.

To build mock samples with line EW that does not correlate with the X-ray luminosity, we first assign a constant line EW to all AGNs in our sample, and apply a Gaussian scatter to the EW for each source (in log space, with $\sigma_{\rm rms}$EW measured by normalizing the observed EW of the "*per source*" results to the best-fitting line, see Fig. 7(c) in Paper I), to account for the intrinsic scatter in EW distribution. Random continuum variations were then added to the luminosity for each source. To match the observed "*per source*" sample in Paper I, multiple observations of individual sources were simulated and their luminosities were then

averaged. Such simulation was repeated for each source to build 10,000 artificial samples. Figure 3(a) shows the distribution of the best-fit slopes (solid line) for the artificial samples. It can be seen that ∼8% simulations can produce steeper anti-correlation than that was observed ($\alpha = -0.11 \pm 0.03$), consistent with the results of Jiang et al. (2006).

Recent observations of some highly variable narrow line Seyfert 1 galaxies and X-ray binaries revealed that some of them show lognormal X-ray flux distribution (e.g., Gaskell et al. 2004; Uttley et al. 2005). To better match the observations, it is worth considering the model of lognormal variability in our simulations, in addition to the above Gaussian luminosity distribution. Because the $F_{\rm var}$ was calculated in linear space, the Gaussian width in log space was replaced by the formula $\sigma = \sqrt{ln(1 + F_{\rm var}^2/2)}$. We again built 10,000 artificial samples, and the resulting distribution of the best-fit slopes is shown by the dot-dashed line in Figure 3 (a). It can be seen that, when using the lognormal X-ray continuum variations, the distribution of the slopes from the simulated datasets moves slightly rightwards, with ∼3% of the simulations being able to produce the anti-correlation slopes steeper than the observed value.

The lower panel in Figure 3 shows the distribution of the slopes from the simulations of the "*per observation*" sample. The solid and dot-dashed lines represent the distribution of the simulated anti-correlation slopes with the Gaussian and lognormal continuum variation models, respectively. We see results consistent with that of the "*per source*" simulations, that ∼11% of the simulations with Gaussian variation model can produce slopes steeper than the observed value ($\alpha = -0.18 \pm 0.03$), while the lognormal model can only yield a fraction of ∼3%.

As noted by Markowitz & Edelson (2004), limitations exist when one uses the excess variance as a description of the intrinsic X-ray variability, since each light curve contains independent underlying stochastic process, and there would be significant random fluctuations in the measured variance. In addition, they found the strength of the X-ray variability tends to be different on different timescales and/or at different energy bands. With these caveats in the mind, we investigated the effect of different variability amplitudes on the simulations. Figure 4 shows distributions of the best-fit slopes of the simulated "*per source*" samples, with different variability amplitudes employed. It can be seen that the distribution of the simulated slopes moves towards much steeper values with increasing variability amplitudes. If the variability amplitude is increased by 50%, ∼27% of the simulations (Gaussian variation model) could produce anti-correlation slopes greater than the observed X-ray Baldwin effect, and the mean value is 0.07 ± 0.04, comparable with the observed value of 0.11 ± 0.03 within uncertainties. In the case of lognormal variation model, the fraction also increases from 3% to 9%.

4. CONCLUSIONS

In this paper, we presented a systematic study on the narrow Fe Kα line Baldwin effect in AGNs observed with the *Chandra* high energy grating. By normalizing the line EWs and continuum luminosities to the time-averaged values for AGNs with multiple HEG observations, we found a strong anti-correlation between both quantities with a best-fitting slope of -0.82 ± 0.10, statistically consistent with a slope of -1. This result indicates generally that the flux of the Fe Kα line of an individual AGN in *Chandra* grating sample is nearly constant and lacks a corresponding response to the continuum variation. We simulated the X-ray continuum variation to test the possibility whether such observational bias could totally account for the observed X-ray Baldwin effect. We find that the simulations could yield significant anti-correlation between EW and continuum luminosity, and the strength of the simulated Baldwin effect is sensitive to the X-ray variation model and variation amplitude. Based on our HEG sample and current knowledge of AGN's X-ray variation, the possibility that the observed X-ray Baldwin effect is totally an observational bias due to X-ray variation cannot be ruled out. This bias should be taken into account before any scientific conclusion can be made based on an observed X-ray Baldwin effect. One should endeavor to make as many repeated observations of each AGN as possible, covering the relevant timescales, and averaging the results. This could minimize the bias and help us to reveal the underlying intrinsic X-ray Baldwin effect, if there is any.

X.W.S. thanks the support from China postdoctoral foundation. We acknowledge support from Chinese National Science Foundation (Grant No. 10825312, 11103017), and the Fundamental Research Funds for the Central Universities (Grant No. WK2030220004, WK2030220005). This research made use of the HEASARC online data archive services, supported by NASA/GSFC. The authors are grateful to the *Chandra* instrument and operations teams for making these observations possible.

REFERENCES

Bianchi S., La Franca F., Matt G., et al. 2008, MNRAS, 389, 52

Bianchi S., Guainazzi M., Matt G., & Fonseca Bonilla, N., 2007, A&A, 467, L19

Chaudhary, P., Brusa, M., Hasinger, G., Merloni, A., & Comastri, A. 2010, A&A, 518, 58

Fukazawa, Y., Hiragi, K., Mizuno, M. et al. 2011, ApJ, 727, 19

Gaskell, C. M. 2004, ApJ, 612, L21

Guainazzi M., Bianchi S., Dovčiak M., 2006, AN, 327, 1032

Iwasawa, K., & Taniguchi, Y. 1993, ApJ, 413, L15

Jiang, P., Wang, J. X., & Wang, T. G. 2006, ApJ, 644, 725

Jiang, P., Wang, J. X., & Shu, X. W. 2011, ScChG, 54, 1354

Jiménez-Bailón, E., Piconcelli, E., Guainazzi, M. et al. 2005, A&A, 435, 449

Kaspi, S., Brandt, W. N., Netzer, H. et al. 2000, ApJ, 535, L17

Krumpe, M., Lamer, G., Markowitz, A., & Corral, A. 2010, ApJ, 725, 2444

Lubiński P., Zdziarski A. A., 2001, MNRAS, 323, L37

Liu, T., & Wang, J. X. 2010, ApJ, 725, 2381

Markert T. H., Canizares C. R., Dewey D., McGuirk M., Pak C., Shattenburg M. L., 1995, Proc. SPIE, 2280, 168

Markowitz, A., & Edelson, R. 2004, ApJ, 617, 939

Nandra, K., George, I. M., Mushotzky, R. F., Turner, T. J., & Yaqoob, T. 1997a, ApJ, 476, 70

Nandra, K., George, I. M., Mushotzky, R. F., Turner, T. J., & Yaqoob, T. 1997b, ApJ, 488, 91

Nandra K., 2006, MNRAS, 368, L62

Nandra, K., O'Neill, P. M., George, I. M., & Reeves, J. N. 2007, MNRAS, 382, 194

Nayakshin, S. 2000a, ApJ, 534, 718

Nayakshin, S. 2000b, ApJ, 540, L37

Page, K. L., O'Brien, P. T., Reeves, J. N., & Turner, M. J. L. 2004, MNRAS, 347, 316

Perola G. C., Matt G., Cappi M. et al. 2002, A&A, 389, 802

Shu X. W., Yaqoob T. & Wang J. X. 2010, ApJS, 187, 581 (Paper I)

Shu X. W., Yaqoob T. & Wang J. X. 2011, ApJ, 738, 147

Sulentic J. W., Marziani P., Zwitter T., Calvani M., Dultzin-Hacyan, D., 1998, ApJ, 501, 54

Uttley, P., McHardy, I. M., & Vaughan, S. 2005, MNRAS, 359, 345

Weaver K. A., Gelbord J., Yaqoob T., 2001, ApJ, 550, 261

Winter L. M., Mushotzky R. F., Reynolds C. S., Tueller J., 2009, ApJ, 690, 1322

Yaqoob T., George I. M., Nandra K., Turner T. J., Serlemitsos P. J., Mushotzky R. F., 2001, ApJ, 546, 759

Yaqoob T., George I. M., Kallman T. R., Padmanabhan U., Weaver. K. A., Turner T. J., 2003, ApJ, 596, 85

Yaqoob T., Padmanabhan U., 2004, ApJ, 604, 63

Yaqoob, T., Reeves, J. N., Markowitz, A., Serlemitsos, P. J., & Padmanabhan, U. 2005, ApJ, 627, 156

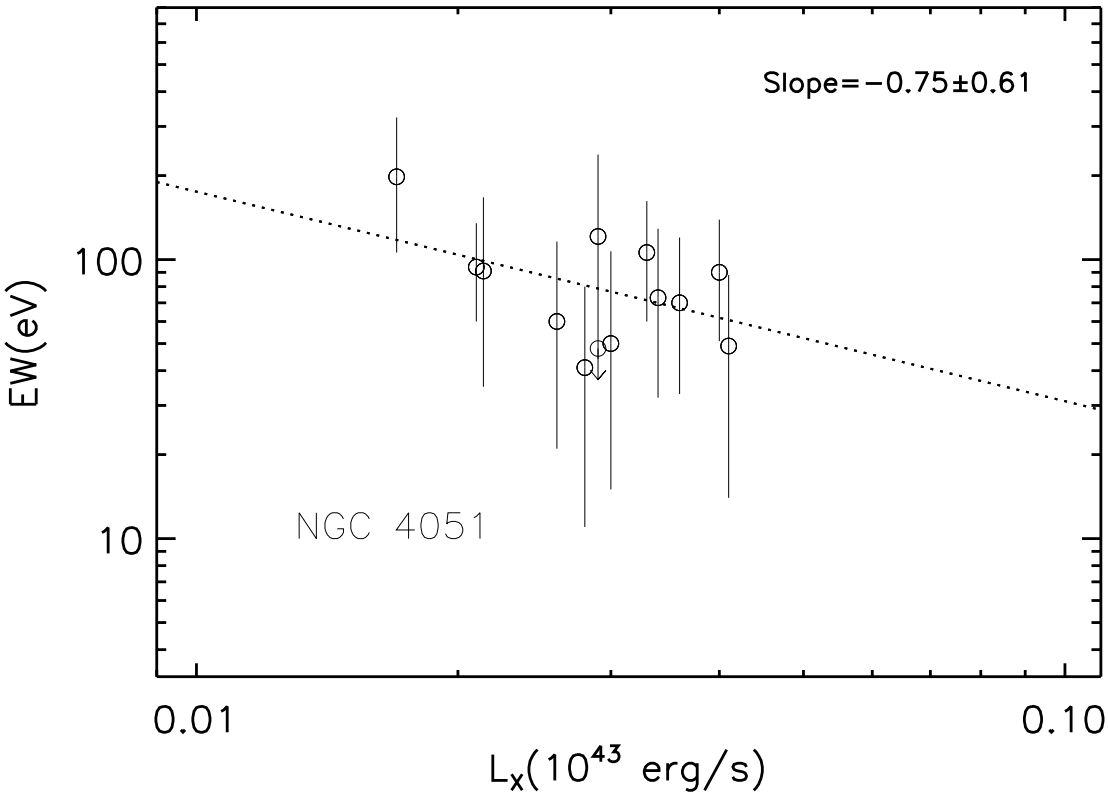

Fig. 1.— 15 *Chandra HETGS* observations of NGC 4051, which show a clear inverse correlation between the narrow Fe Kα line EW and the 2–10 keV luminosity, with a very steep relationship $EW \propto L_x^{-0.75\pm0.61}$ (dotted line).

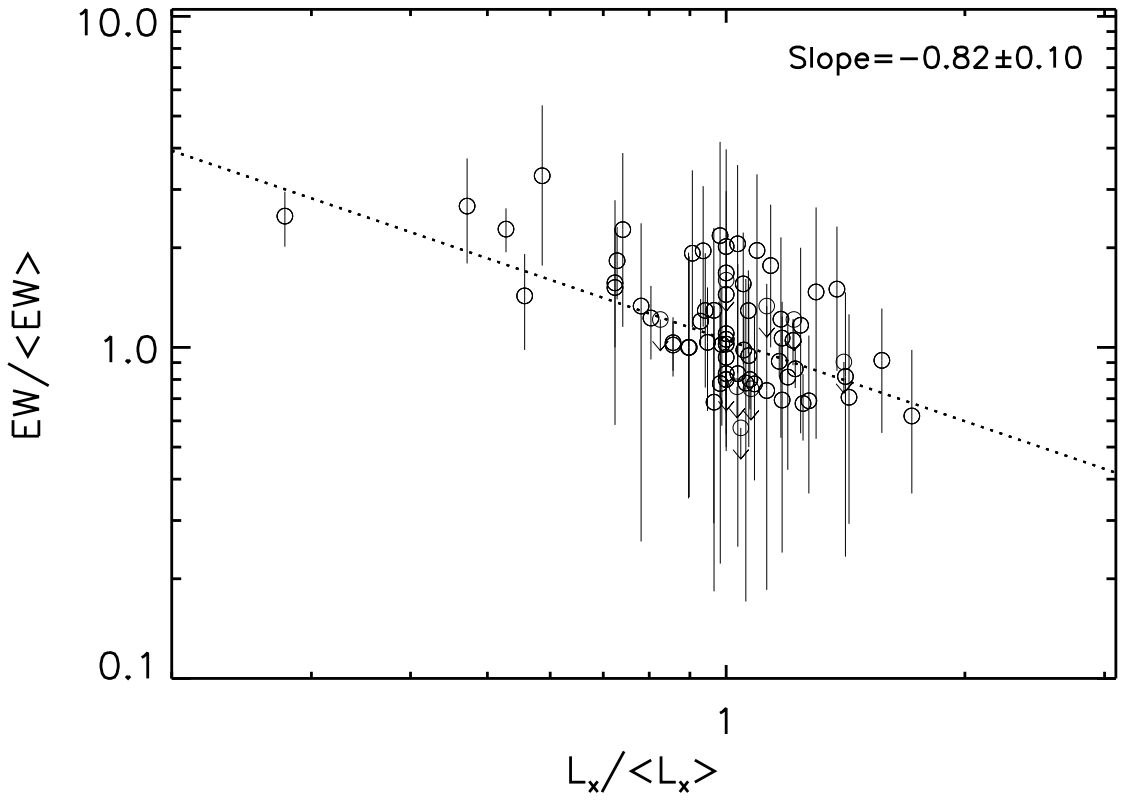

Fig. 2.— Relation between the Fe Kα line EW and the X-ray luminosity, both normalized by their time-averaged values for sources which were observed more than once by *Chandra* HEG. The time-averaged EW ($\langle EW \rangle$) and X-ray luminosity ($\langle L_x \rangle$) are from the spectral fitting of the time-averaged spectrum for each source (see Paper I for details). The dotted line shows the best fit to the data: $EW \propto L_x^{-0.82\pm0.10}$.

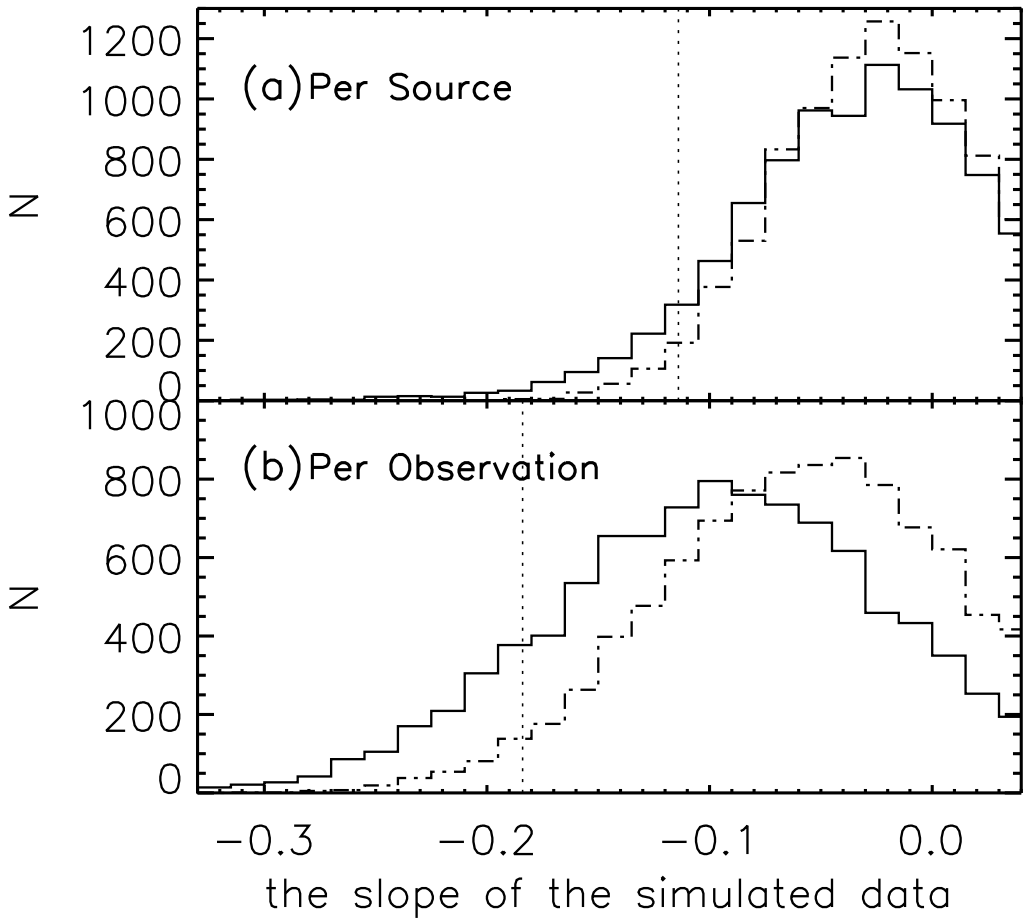

Fig. 3.— Distribution of the best-fit slopes of log EW versus log L_x of the simulated datasets. *Panel (a)*: histogram of the simulated power-law slopes for "*per source*" results. *Panel (b)*: as (a), but for "*per observation*" sample. The solid lines represent distributions assuming the variability is normally (or Gaussian) distributed in the simulations, while dot-dashed lines are for the variability with lognormal distribution. The vertical dotted lines show the observed slopes for each sample, which are -0.11 ± 0.03 and -0.18 ± 0.03, respectively.

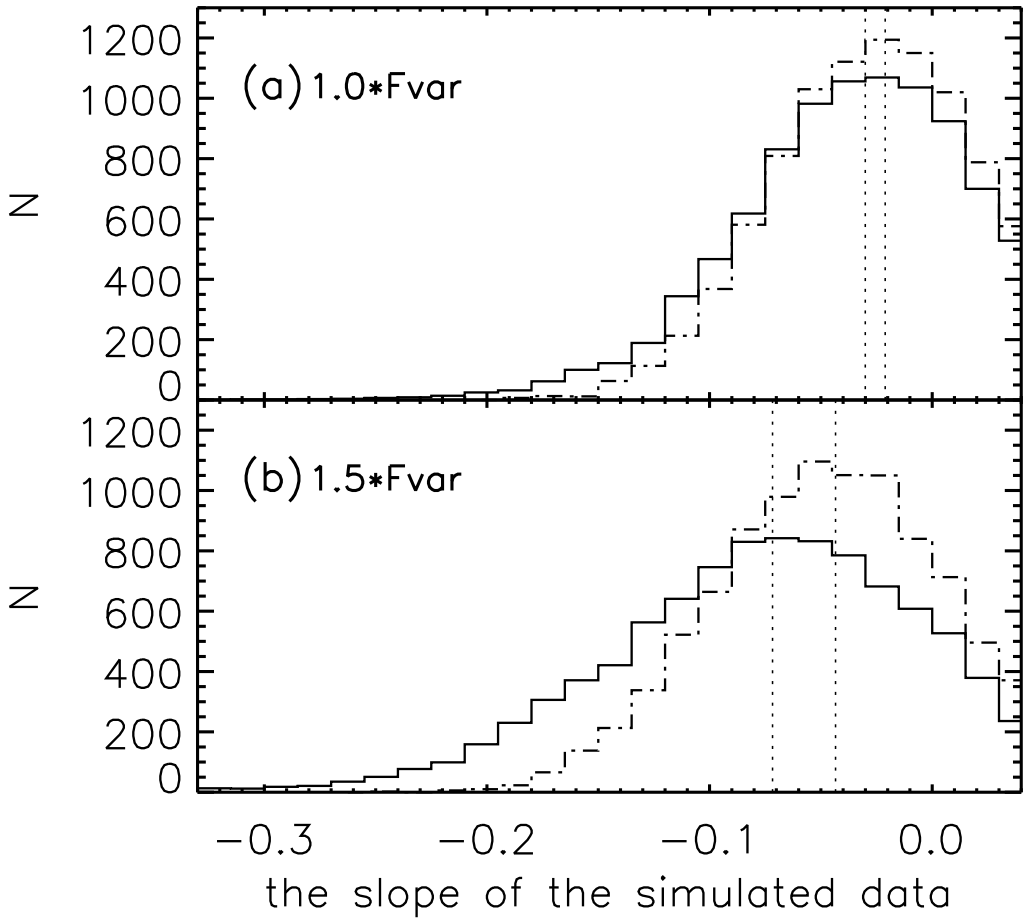

Fig. 4.— Distribution of the best-fit slopes of $\log EW$ versus $\log L_x$ for the simulated "*per source*" sample. The lower panel corresponds to an increase of fractional variability amplitude (F_{var}) by 50%. The solid and dot-dashed lines represent different time variation model, as shown in Figure 3. The vertical dotted lines show the means of the slope for each distribution.